UDC 551.583.15:551.513.7:551.542(215-17)

LARGE-SCALE FEATURES OF MONTHLY MEAN NORTHERN HEMISPHERE ANOMALY MAPS OF SEA-LEVEL PRESSURE

JOHN E. KUTZBACH

Department of Meteorology, The University of Wisconsin, Madison, Wis.

ABSTRACT

Spatial patterns of circulation variability over the Northern Hemisphere and their changes during the past 70 yr (1899–1969) are examined using eigenvector analyses of mean January and July sea-level pressure maps. The first several eigenvectors display variability associated with the major centers of action (the subpolar oceanic Lows, the subtropical oceanic Highs, the winter Siberian High, and the summer Asiatic Low). The pattern of the first eigenvector of January suggests that the intensity and latitudinal position of the major circulation features over the North Atlantic are associated with the intensity and position of the Aleutian Low over the North Pacific.

The time series of the coefficients of the hemispheric eigenvectors are used to identify intervals of change in the hemispheric circulation associated with features on the scale of the major centers of action. These time series provide a more general description of circulation change than that obtained from local or regional indices; but at the same time, they provide more detailed information than time series of hemispherically averaged indices. Two intervals of change in the large-scale hemispheric circulation are identified: the early to mid-1920s and the early to mid-1950s. Of the three periods separated by these two intervals of change, maximum contrast is noted between the first and third. For January, the strongest circulation features are found in the North Atlantic and European sectors in the first (earliest) period and in the North Pacific and Asian sectors in the third (latest) period.

1. INTRODUCTION

A variety of numerical indices have been used to characterize the monthly mean atmospheric circulation and study its year-to-year changes. Zonal and meridional pressure gradients, pressure gradients between identifiable circulation features, trough and ridge positions, and locations and intensities of circulation features may be mentioned as examples of local and regional indices (Lamb and Johnson 1966). Although these indices are very useful for regional studies, it is difficult to combine them into a comprehensive and quantitative picture of the large-scale circulation variability in space and time. On the other hand, the use of zonally averaged indices, such as north-south pressure profiles (Willett 1965) or globally averaged indices, such as world mean temperature, reduce or eliminate information on the scale size of circulation variability.

The purpose of this paper is to examine the spatial patterns of circulation variability over the Northern Hemisphere and their changes during the past 70 yr using eigenvector analyses of the sea-level pressure field. Eigenvector analysis, like various forms of harmonic analysis, permits the decomposition of patterns into components. Unlike harmonic components, the eigenvectors (also referred to as principal components or empirical orthogonal functions) have no predetermined forms. Rather, their forms may resemble observed and recurrent patterns of the variable being analyzed. In this study, the eigenvector patterns reflect the tendency for preferred configurations of the large-scale "centers of action." Several spatial patterns of circulation variability on the scale of the major centers of action are described. The time series of the coefficients of the hemispheric eigenvectors are then used to identify times of change in the hemispheric circulation associated with these space scales.

The data and analysis techniques are described in sections 2 and 3. The main results are found in sections 4 and 5.

2. THE DATA

January and July monthly mean sea level pressure maps were used in the analyses. The January (July) series covered the period 1899–1969 (1899–1968) and was obtained from the Extended Forecast Division of ESSA (Environmental Science Services Administration) at Suitland, Md.; data for the years 1940 (1939) through 1944 were not available for large regions of the hemisphere, and these years were omitted leaving a total of 66 (64) monthly mean maps. The 180-point network used in the eigenvector analysis is indicated by dots in figure 1a. Approximately 2 percent of the observations were missing. Linear interpolation was used to replace single or double missing observations. Larger gaps were filled with data from other sources (Lamb and Johnson 1966) after which any irregularities at boundaries between the two analyses were smoothed. It is recognized that uncertainties concerning the original analyses exist, both in oceanic regions at high and low latitudes due to lack of sufficient observations and also in regions of high elevations due to difficulties associated with the reduction of station pressure to fictitious sea-level pressure.

3. EIGENVECTOR ANALYSIS

Reference is made to Sellers (1968), Craddock and Flood (1969), and Kutzbach (1967) for recent discussions of eigenvector analysis techniques, including the various

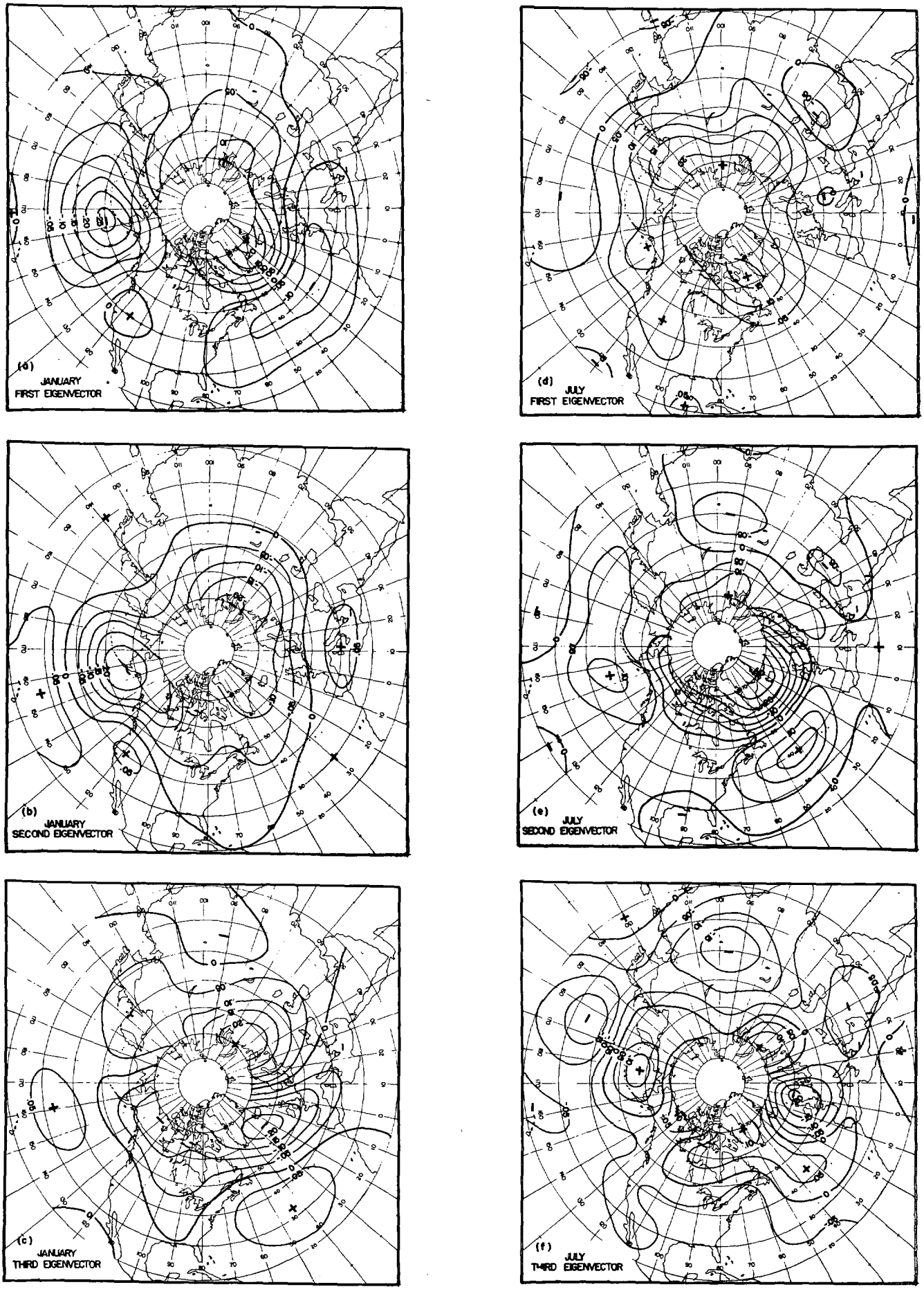

FIGURE 1.—Eigenvectors for January, (a) first, (b) second, and (c) third; eigenvectors for July, (d) first, (e) second, and (f) third. The 180-point network is indicated by dots in (a).

relations stated below, and their application to climatological problems. In addition, Gilman (1957) has used eigenvectors obtained from hemispheric sea-level pressure fields in long-range statistical prediction experiments. The present work may be viewed as an extension of his research to the study of climatic fluctuations and circulation changes. In this study, eigenvalues (λ) and their associated eigenvectors ($\mathbf{e}$) were obtained from a symmetric matrix ($N^{-1}\,\mathbf{FF}'$) describing all possible spatial covariance relationships within the defined network of points for the period treated. Here $\mathbf{F}$ is the M by N observation matrix whose nth column vector ($\mathbf{f}_n$) contains the M observations of sea-level pressure anomalies for the nth year. The anomalies are defined as the departures from the mean map of the N years. For later use, a number of relations are given; first, $\mathbf{f}_n$ can be expressed as a linear combination of the eigenvectors

$$\mathbf{f}_n=\sum_{i=1}^{M} c_{in}\mathbf{e}_i \quad n=1,\ldots,N$$

where c_{in} will be referred to as the coefficient associated with the ith eigenvector for the nth year. Just as the eigenvectors are orthogonal functions of space, the coefficients are orthogonal functions of time. The sum of squares of the coefficient associated with the ith eigenvector $\left(\sum_{n=1}^{N} c_{in}^2\right)$ equals the total variance explained by the ith eigenvector. Finally, two measures of association between observation vectors and eigenvectors will be used. The first is the correlation coefficient r_{in} between $\mathbf{f}_n$ and $\mathbf{e}_i$ or its square r_{in}^2 that represents the fraction of the variance of the nth observation explained by the ith eigenvector. The second is the quantity v_{in}^2 that represents the fraction of the sum of squares of the nth observation vector accounted for by the ith eigenvector; $v_{in}^2=c_{in}^2 \times(\mathbf{f}_n'\,\mathbf{f}_n)^{-1}$. Both measures of association are discussed by Sellers (1968).

The latitudinal distribution of points (18 at 70° N. and 60° N., 36 at 50° N., 40° N., 30° N., and 20° N.) represents a compromise between the desirability of giving equal weight to equal areas and the desirability for greater resolution of features in high latitudes. While the analyses described below were performed on the 180- point network ($M=180$), calculations were also made on a 60-point network ($M=60$) consisting of every third point of the larger network. The only significant difference between the resulting sets of eigenvector patterns was that features could be more accurately located on the 180-point network. For calculations using the 180-point network, it was computationally convenient to first solve for the eigenvalues (λ_a) and associated eigenvectors ($\mathbf{e}_a$) of the N by N cross-product matrix ($N^{-1}\mathbf{F}'\mathbf{F}$). Then the 180-point eigenvectors were obtained using the linear transformation $\mathbf{e}=(N\lambda_a)^{-1/2} \times\mathbf{F}\mathbf{e}_a$ (Hirose and Kutzbach 1969).

The use of anomalies instead of normalized anomalies insures that eigenvector patterns reflect the real spatial distribution of variance over the network. This has the advantage that the patterns can be viewed as being analogous to mean anomaly maps, from which it is possible to infer anomalous mean pressure gradients and winds. It has the disadvantage that the most important eigenvectors tend to describe relationships in areas of maximum variance. In practice, this means that middle- and high-latitude features are emphasized in this study since variability is greatest in these regions. This problem could be avoided by using normalized data, but then the eigenvector patterns would be analogous to normalized anomaly maps and would be more difficult to interpret.[1]

TABLE 1.—*Percent variance explained by each of the first 10 eigenvectors and cumulative explained variance*

Eigenvector	January		July	
	% variance	% cum. variance	% variance	% cum. variance
1	22.0	22.0	15.4	15.4
2	14.6	36.6	10.2	25.6
3	11.7	48.3	9.0	34.6
4	8.7	57.0	7.1	41.7
5	7.0	64.0	5.8	47.5
6	5.2	69.2	5.5	53.0
7	5.1	74.3	4.7	57.7
8	3.4	77.7	4.0	61.7
9	3.2	80.9	3.2	64.9
10	2.9	83.8	3.1	68.0

The variance aud cumulative variance explained by the first 10 eigenvectors, expressed in percent of total variance, are presented in table 1. These figures represent averages for the entire network. The spatial patterns of explained variance show considerable variability. The latitudinal variability of cumulative explained variance and total variance is presented in table 2. As noted above, cumulative explained variance is large where variance is large. It varies from 80 to 90 percent in high latitudes to 40 to 50 percent in low latitudes. The small values of cumulative explained variance at low latitudes indicate that variability at these latitudes is not uniquely associated with the much greater variability at high latitudes.

The explained variance is distributed among a large number of eigenvectors (table 1), thus illustrating the diversity of anomaly maps in different years. However, only the first several eigenvectors are frequent primary components of individual anomaly maps. The term primary component is used here to denote the eigenvector that explains the largest fraction of the variance of an individual anomaly map. The amount of variance explained by the primary component ranges from 15 to 65 percent and averages over 30 percent for January and 25 percent for July. Secondary and tertiary components

[1] Eigenvectors were obtained from normalized data (using the 60-point network) for comparison with those obtained by Gilman (1957). Although the number of years and the method of solution were very different for the two studies, the results were similar, especially for the first several eigenvectors.

TABLE 2.—*Latitudinal distribution of* (A) *cumulative variance explained by the first 10 eigenvectors (in percent) and* (B) *variance (expressed as percent of total variance)*

Latitude (° N.)	A		B	
	Jan.	July	Jan.	July
70	89.8	80.6	22.4	22.6
60	89.9	84.8	19.6	20.8
50	78.6	64.4	30.5	23.0
40	69.0	64.4	18.0	16.0
30	54.0	53.0	7.0	9.8
20	43.8	44.2	2.5	7.8

TABLE 3.—*Number of times the first 10 eigenvectors were primary, secondary, or tertiary components (1, 2, 3), also the number of times* $|r_{in}| > 0.5$

Eigenvector	Jan.				July			
	1	2	3	$\lvert r_{in}\rvert>0.5$	1	2	3	$\lvert r_{in}\rvert>0.5$
1	24	13	2	24	16	10	6	8
2	13	13	5	13	13	12	4	6
3	12	9	5	11	12	6	8	4
4	4	11	8	5	6	7	6	3
5	6	2	12	6	5	3	11	3
6	2	6	6	3	2	3	6	3
7	3	7	9	2	4	6	6	0
8	1	3	4	1	1	10	5	0
9	1	1	5	1	3	2	1	0
10	0	1	6	0	2	5	3	1

explain progressively less variance.[2] A count of the number of times that eigenvectors are primary, secondary, and tertiary components of individual maps is presented in table 3. For example, the first eigenvector of January is the primary component 24 times, secondary 13 times, and tertiary 2 times. In contrast, the corresponding counts for the 10th eigenvector are 0, 1, and 6. Table 3 also contains a tally of the number of times the correlation coefficient between the eigenvectors and the anomaly maps, r_{in}, exceeds ± 0.5. Attention will be mainly restricted to the first three eigenvectors of January and July (fig. 1) in the remainder of the paper because of the frequency with which they are primary components of individual anomaly maps.

Several comments will be made before describing the patterns. First, it has already been emphasized that the eigenvector patterns are only components of the monthly mean anomaly maps. Only occasionally does an eigenvector explain more than 50 percent of the variance of an individual map (table 4). Even then, it is probable that the large-scale circulation within the month is not homogeneous and that the resulting mean map is an average of two or more circulation regimes. In addition, large-scale features of mean maps result partly from transient smaller scale phenomena that are entirely absent from mean maps. Thus, these patterns are not hemispheric weather "types." Nevertheless, it is often possible for synoptic meteorologists and climatologists to infer many characteristics of daily synoptic developments and likely mean temperature and precipitation patterns from examination of mean maps. At least in certain cases, it appears that these diagnostics can be made objective using eigenvector analysis (Kutzbach 1967). Second, each eigenvector pattern actually represents two patterns, since its associated coefficient determines the sign of its departures. It is known that there is a tendency for maps with opposite large-scale anomalies to have the same features (except for sign reversals); see, for example, Martin (1953). However, there are always some differences since many different climatological factors are active (and not reversible). Therefore, the eigenvector patterns depict a rather blurred average of actual maps with their various positive and negative anomaly features. Third, one may inquire as to whether physical interpretation is further complicated by the fact that eigenvectors are constrained to be orthogonal to one another. That is, while the first eigenvector is chosen to have highest resemblance to all observation vectors ($\mathbf{f}_n$) simultaneously, the second is chosen to have highest resemblance to the residuals, that is, to components of the observation vectors that are orthogonal to the first eigenvector, and so on. For the January sample, it was possible to examine

TABLE 4.—*Objective measures of resemblance (r^2 and v^2) between eigenvectors and observation vectors for particular years*

Jan. First eigenvector						July First eigenvector					
Minus			Plus			Minus			Plus		
Year	r^2_{1n}	v^2_{1n}	Year	r^2_{1n}	v^2_{1n}	Year	r^2_{1n}	v^2_{1n}	Year	r^2_{1n}	v^2_{1n}
1909	0.25	0.29	1931	0.48	0.51	1924	0.42	0.47	1899	0.26	0.28
1910	.31	.33	1936	.58	.60	*1926	.45	.47	*1918	.51	.46
1911	.41	.45	1939	.30	.32	1935	.35	.30	1922	.38	.54
*1916	.60	.63	*1945	.63	.60	1947	.36	.31	1962	.42	.27
1923	.30	.30	1958	.51	.53						
1925	.27	.27	1960	.60	.55						
1932	.39	.40	1961	.42	.45						
1949	.30	.30	1965	.38	.41						
1957	.56	.54	1966	.49	.51						

Second eigenvector						Second eigenvector					
Minus			Plus			Minus			Plus		
Year	r^2_{2n}	v^2_{2n}	Year	r^2_{2n}	v^2_{2n}	Year	r^2_{2n}	v^2_{2n}	Year	r^2_{2n}	v^2_{2n}
1907	0.32	0.38	1908	0.31	0.24	1902	0.28	0.28	1920	0.37	0.36
1950	.34	.33	1914	.26	.32	*1907	.49	.46	*1938	.40	.38
1954	.29	.28	1926	.28	.34	1968	.36	.34	1959	.24	.24
1956	.35	.26	*1928	.47	.47						
1968	.40	.37	1946	.36	.36						
*1969	.59	.59	1964	.42	.45						

Minus or plus indicates the sign of the eigenvector's coefficient; the asterisk marks the year of highest resemblance.

[2] For January (July), linear combinations of from one to four eigenvector patterns explain from 60 (45) percent to 75 (65) percent of the variance of the individual maps. Combinations of three eigenvectors explain an average of 65 (50) percent of the variance implying correlations on the order of ± 0.8 (0.7) between actual anomaly maps and maps constructed from the correctly weighted linear combinations of three eigenvectors.

this question by removing the 10 maps that correlated best with the first eigenvector (fig. 1a) and repeating the analysis using the reduced observation matrix. It was found that the new "first" eigenvector was a close copy of the original second eigenvector (fig. 1b), thus suggesting that its features were not distorted by the orthogonality constraint. It was not practical to continue this procedure since the observation matrix would have become too small. This test was not applied to the July data; however, the broadly circular disposition of isolines in the first eigenvector (fig. 1d) suggests that any spatial distortions in the pattern of the second eigenvector (fig. 1e) produced by the orthogonality constraint would be quite minor. Thus, at least the first two eigenvector patterns of both January and July isolate features that are frequent and recognizable components of individual anomaly maps during the period studied.

4. SPATIAL EIGENVECTOR PATTERNS

In the following paragraphs, the most significant features of the eigenvector patterns are described. For the first two eigenvectors, descriptions are provided of the general appearance of actual mean maps for individual years in which the eigenvector patterns most closely resemble the actual anomaly maps. Both the years and the corresponding objective measures of resemblance are presented in table 4. Alternate descriptions are sometimes given because different features are emphasized in different years—even though the overall resemblance as measured by the two indices (r^2_{in} and v^2_{in}) might be similar. Even so, the descriptions are not strictly accurate for all years. All references to mean conditions refer to the mean over the period of this study. Descriptions of eigenvector patterns are given in terms of the sign shown on the illustrations, it being understood that all signs are reversed if the coefficient associated with the eigenvector has a negative sign.

First eigenvector for January (fig. 1a). There are two areas of large departure of opposite sign in the Atlantic. In the north, a region of positive departures is centered slightly north of the mean position of the Icelandic Low. This feature apparently extends across the Pole and south over northern Russia to the east of Novaya Zemlya. In the south, an elongated pattern of negative departures extends from the eastern United States to central Europe with maximum departures along 40° N. in the mid-Atlantic, well north of the mean center of the Atlantic High. A large negative departure in the northern Pacific is centered near 50° N., 165° W., clearly east of the mean position of the Aleutian Low. While explaining 22 percent of the total variance, this pattern explains 30 to 50 percent of the variance at points in the North Atlantic and North Pacific located within the regions of large departure.

a. Features of actual maps (negative coefficient): strong Icelandic Low near or slightly north of its mean position with westerly flow extending northeast toward Novaya Zemlya; continuous band of high pressure across the Atlantic with axis of highest pressure somewhat north of mean; Aleutian Low often split into two centers, the one west of its mean position near Kamchatka and the other in the Gulf of Alaska; sometimes the latter feature is entirely absent and replaced by a High extending south from Alaska over the gulf.

b. Features of actual maps (positive coefficient): Icelandic Low weak or displaced far south, or split into two centers, one west of the southern tip of Greenland, the other in the Norwegian Sea; pressures higher than mean over Greenland; Atlantic High weak and shifted south; Aleutian Low strong and often extended south and east of its mean position, or split with one center in the Gulf of Alaska and another center to the west.

Second eigenvector for January (fig. 1b). The eigenvector resembles a wave number 3 pattern with troughs at 65° E., 160° W., and 50° to 60° W. in midlatitudes. The most intense negative departures are over northern Russia and Alaska. A weaker trough of negative departures extends southwest from Iceland toward the West Indies.

a. Features of actual maps (negative coefficient): pressures higher than mean across parts of Scandinavia and northern Russia, sometimes a closed High is located in this sector; High located over Alaska with ridge of high pressure extending southeast into the Canadian Prairies.

b. Features of actual maps (positive coefficient): cyclonic circulation associated with the Icelandic Low extends farther northeast than in the mean, sometimes the center of lowest pressure is as far east as Novaya Zemlya; Aleutian Low displaced north and east of its mean position toward the southern coast of Alaska.

The third eigenvector (fig. 1c) has a region of negative departures north of 50° N. extending from Alaska eastward to Scandinavia with centers of maximum departure over northwestern Canada, Greenland, and just south of Iceland. A center of positive departures near Novaya Zemlya extends south toward the Caspian Sea. Centers of maximum positive departures are found in both oceans, south and west of the centers of negative departure in high latitudes. This suggests blocking patterns near the west coasts of North America and Europe when the eigenvector's coefficient is negative.

First eigenvector for July (fig. 1d). An area of positive departures covers the polar cap with four protrusions into midlatitudes—these are centered in the Davis Strait, over northern Russia and northeastern Siberia, and in the Gulf of Alaska. A weak but broad region of negative departures covers most of the central and western Pacific south of 40° N. An intense but small area of negative departures is centered near the Caspian, north and west of the mean center of the monsoon Low.

a. Features of actual maps (negative coefficient): pressures generally lower than mean in northern latitudes; Low in the Davis Strait; broad area of low pressure over Asia extends farther north than in the mean; closed Lows sometimes located along the northern coast of Asia.

b. Features of actual maps (positive coefficient): pressures generally higher than mean in northern latitudes; weak Low (if any) in the Davis Strait; closed Highs located along the northern coast of Asia.

Second eigenvector for July (fig. 1e). A large area of negative departures centered over eastern Greenland is

the strongest feature of the pattern. This imparts a definite asymmetry toward the Atlantic sector in northern latitudes. Over both oceans, regions of positive departures are centered somewhat north of the mean axes of the summer anticyclones. Although this eigenvector accounts for only about 10 percent of the total variance (table 1), it accounts for 40 percent of the variance or more at certain points in the North Atlantic located within the regions of large departure.

a. Features of actual maps (negative coefficient): higher than mean pressures over the Arctic Archipelago, Greenland, and/or adjacent waters; any Lows in this sector are either very weak or shifted south of their mean locations; oceanic anticyclones are weaker and shifted south of their mean positions.

b. Features of actual maps (positive coefficient): no High over Greenland or the adjacent waters; Lows in this sector stronger than mean and shifted north; oceanic anticyclones strong and extended farther north than in the mean.

The third eigenvector (fig. 1f) has three pairs of departure centers of opposing signs: a negative departure located north of the British Isles and a positive one to the west; a positive departure located south of Novaya Zemlya and a large negative one to the southeast over the Tibet Plateau; a positive departure located in the Bering Sea and a negative one to the southwest in the mid-Pacific. More than 40 percent of the total variance is accounted for at certain points located within the areas of negative departure over the Tibet Plateau and the mid-Pacific.

For both months, the scale size of features in the eigenvector patterns tends to decrease with increasing eigenvector number. However, the decrease is irregular. Some large-scale patterns are found in higher order eigenvectors.

Patterns similar in broad respects to portions of those described here have received attention in studies of physical mechanisms of circulation variability. Lamb and Johnson (1959) have noted that latitudinal shifts of circulation features tend to be more pronounced in the North Atlantic than elsewhere and have suggested possible reasons linking these shifts with the shape of the Atlantic Basin. Namias (1969) has discussed the year-to-year variability of the Aleutian Low and possible causes of this variability. Bjerknes (1962) has described associations between broad scale north-south pressure differences in the North Atlantic (similar to the appropriate sectors of $\mathbf{e}_1$ for January and $\mathbf{e}_2$ for July) and ocean surface temperature patterns. In a more recent discussion of ocean-atmosphere interaction in the Pacific (Bjerknes 1966), the association between an intensified Aleutian Low and downstream intensification of the Greenland High and weakening of the Icelandic Low was noted in the winter of 1957–1958. The actual anomaly pattern for January 1958 bears general resemblance to $\mathbf{e}_1$ (table 4) except for a negative anomaly over Russia. Lamb and Johnson (1959) have noted a similar relation, stating that "when the circulation over the North Pacific is strong, it sometimes happens that warm air is repeatedly advected over North America in such a way as to disturb the development of the Canadian cold trough and thereby suppress the circulation intensity over the North Atlantic." The present study indicates that this pattern (or its negative) is frequently an important component of January anomaly maps.

Latitudinal variability, with departures of opposite sign located in high and low latitudes is a feature of most of the eigenvectors.[3] Oscillation between pressure at high and low latitudes is a well-documented characteristic of the atmospheric circulation in most years (see, for example, Namias 1953). The eigenvector patterns indicate that it is also a characteristic of the year-to-year variability, a fact that has been demonstrated by other analyses. For example, Brier (1968) has shown the tendency for year-to-year oscillations of pressure between high and low latitudes using eigenvector analyses of the zonally averaged pressure profiles. Much earlier, Walker (1932) identified a north-south opposition of pressure departures in the North Atlantic sector, that is, between the Icelandic Low and the Azores High, that closely resembles the Atlantic sector of $\mathbf{e}_1$ for January. He described a similar feature in the Pacific, an opposition between the Aleutian Low and the Pacific High that resembles the Pacific sector of $\mathbf{e}_2$ for January. He noted that these phenomena were best developed in winter and that there was no correlation between them. This latter result applies equally to the present study since the time series of the coefficients associated with $\mathbf{e}_1$ and $\mathbf{e}_2$ are uncorrelated (orthogonal). Walker's failure to note the area of large departures in the North Pacific associated with the north-south opposition in the Atlantic ($\mathbf{e}_1$) can perhaps be attributed to the selection of points in his correlation studies (limited to continental stations and several island stations). Iudin (1967) has reported that the two northern hemispheric oscillations defined by Walker are described by the first eigenvector of the pressure field. His result, obtained from daily pressure fields, differs from the one described here.

5. CIRCULATION CHANGES

Time series of eigenvector coefficients c_1 through c_3 for both January and July are presented in figure 2. The different characteristics of the time series may contain information about physical processes. For example, of the coefficients of the first two eigenvectors for January, the first shows a tendency for departures of the same sign for intervals on the order of a decade or longer, thus suggesting an association of $\mathbf{e}_1$ with slowly changing anomalous energy sources or sinks. The second behaves much more erratically throughout the period, suggesting that $\mathbf{e}_2$ may

[3] However, due to compensatory effects in different longitudinal sectors, the overall zonal index—defined as the pressure difference between 35° N. and 55° N. averaged around the hemisphere—is not necessarily large. Calculating this index from the eigenvector patterns, it was noted that for the first three eigenvectors of January, only the second and third had large zonal indices—the zonal index of the first eigenvector being almost an order of magnitude less than that of either the second or the third. January zonal indices $\mathbf{e}_1$ through $\mathbf{e}_3$, −0.015, 0.100, 0.130, July zonal indices $\mathbf{e}_1$ through $\mathbf{e}_3$, −0.130, 0.077, −0.030.

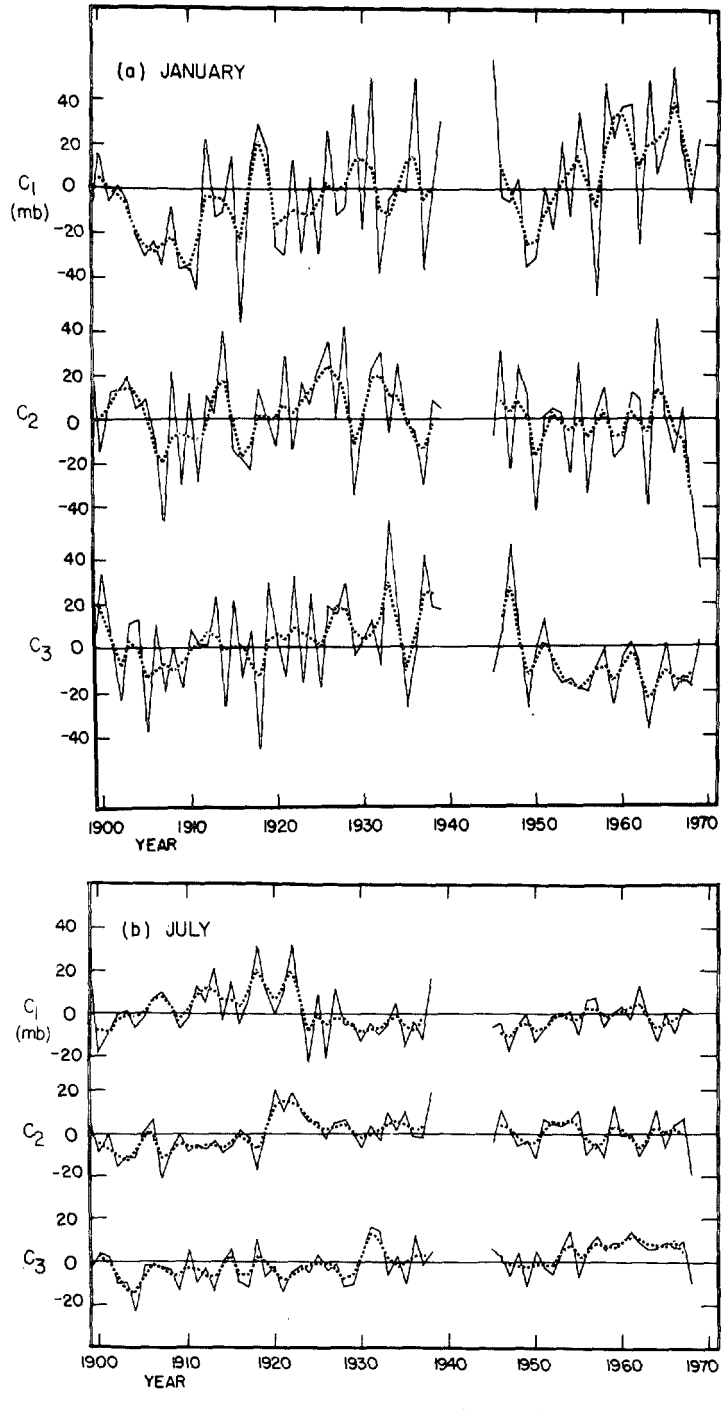

FIGURE 2.—Time series of the coefficients (c_1, c_2, c_3) associated with (a) the first three eigenvectors for January and (b) the first three eigenvectors for July. Units are in millibars. The eigenvectors must be multiplied by the coefficients to obtain spatial departure patterns in millibars. The dotted line represents the filtered series.

reflect variability confined primarily to the atmosphere, or associations with anomalous energy sources and sinks that have little year-to-year persistence.

All series show a tendency for fluctuations with periods of 2 to 3 yr. These are sometimes noticeable for intervals on the order of a decade or longer, but they are never sustained over the entire record (see Brier 1968 for a discussion of quasi-biennial oscillation phenomena as reflected in eigenvectors of zonally averaged monthly mean sea level pressures). Because of the large amount of variability with periods of 2 to 3 yr, a filtered series, obtained by application of a three-term binomial filter (¼, ½, ¼) is also presented. This filter strongly attenuates fluctuations with periods of 3 yr or less.

An attempt was made to identify those times at which the largest changes in circulation patterns occurred by inspecting the time series of the eigenvector coefficients for both January and July. In addition, time series of correlation coefficients between actual anomaly maps and eigenvector patterns (not shown—these series are very similar in appearance to the time series of the coefficients) were examined. The great variability in the details of the time series—and hence the variability of the actual anomaly maps—precludes any precise description. However, two intervals of change are apparent: the early to mid-1920s and the early to mid-1950s. The three periods separated by these two intervals of change are not homogeneous, but the changes appear to be of lesser magnitude or shorter duration. For convenience of discussion, the three periods will be referred to in chronological order as the first, second, and third periods. (The circulation during the missing years of the late 1930s and early 1940s may have been quite different from that which preceded or followed it; but because the missing period is relatively short, its inclusion would probably not materially change the results.)

In January, the coefficient of $\mathbf{e}_1$ is predominantly negative during the first period (fig. 2 and table 4). In the second period, it is frequently important, but there is no sign preference. In the third period, the larger bias toward positive values of its coefficient is apparent. The second eigenvector of January is about equally important in all periods and shows no strong sign preferences throughout the period of study. The third eigenvector tends to have positive coefficients in the second period and negative coefficients in the third. In July, the coefficient of $\mathbf{e}_1$ is predominantly positive in the first period and negative in the second. The coefficient of $\mathbf{e}_2$ is negative in the first period and shows a bias toward positive values in the second period. The coefficient of $\mathbf{e}_3$ is frequently negative in the first period and positive in the third.

For brevity, the time behavior of only the first three coefficient series has been described. Although they account for only 45 percent (35 percent) of the total variance in January (July), they account for a much larger fraction of the variance associated with the large space scales. A more detailed analysis including the first six eigenvectors for each month leads to essentially the same conclusions regarding the identification of times of major circulation change. Also, the first six eigenvectors of the correlation matrix between all 66 (64) anomaly maps of January (July) indicate a similar division.

As noted in the introduction, the specification of times of circulation or climatic change implies some assumptions

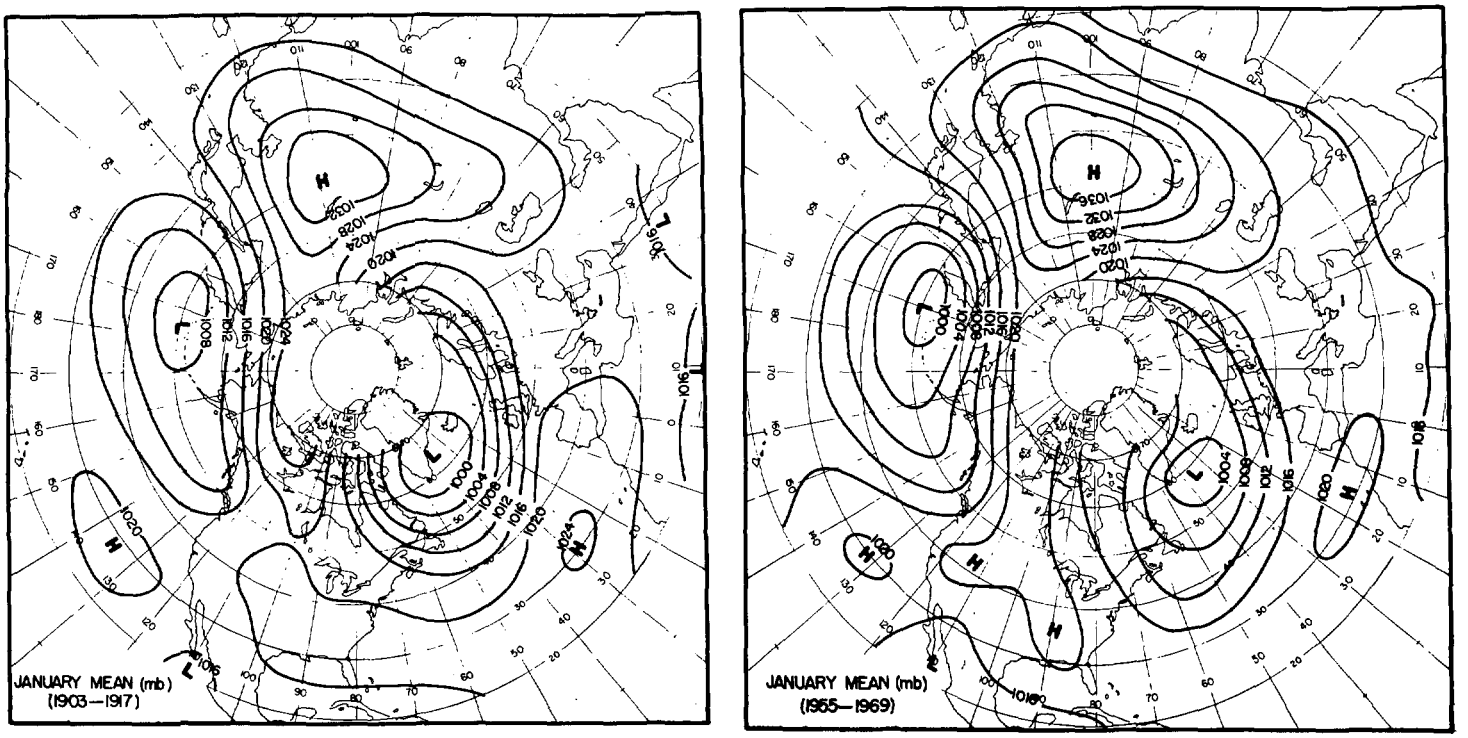

FIGURE 3.—January 15-yr mean sea level pressure patterns from the first period, 1903–1917 and from the third period, 1955–1969.

regarding the scale size of the features being studied. Thus, comparison of the present results, which are based upon changes in circulation features with scale sizes of the centers of action, with results based on local or regional indices on the one hand or globally averaged indices on the other will not be attempted. However, there are many points of similarity between the circulation changes implied by the time variability of the coefficients of the first several eigenvectors and the qualitative descriptions of large-scale circulation changes based upon interpretation of a wide variety of regional indices of circulation variability (Lamb 1966*a*, 1966*b*; Lamb and Johnson 1959; and Bjerknes 1962). Also, Dzerdzeevskii (1966) and Girs (1967) have reported subjective classifications of daily hemispheric pressure maps into hemispheric circulation types and identified changes in type frequencies at approximately the times presented here.

The most striking example of circulation change is indicated by the time series of the coefficient of $\mathbf{e}_1$ for January which suggests a large contrast between the mean January circulations of the first and third periods. To illustrate this contrast, 15-yr mean maps are presented for the periods 1903–1917 and 1955–1969 (fig. 3). The differences between these two maps are primarily those explained by the changed sign of the coefficient of $\mathbf{e}_1$. Note the decreased intensity and southward shift of the Icelandic Low, the increased intensity of the Aleutian Low (particularly its eastward extension), and the increased intensity of the Siberian High in the third period. In comparing the decade mean 1950–1959 with earlier long-term means, Gommel (1963) has also noted the recent tendency for a weakened Icelandic Low and for both the Aleutian and Icelandic Lows to form winter auxiliary cells to the east of the parent cells. Although the long-term changes in the intensity and location of the Icelandic Low and Azores High have been frequently studied, their possible association with long-term changes over the North Pacific have received less attention (see section 4).

The contrast between the Julys of the first and third periods is comparatively small and is explained primarily by the changes in the coefficients of $\mathbf{e}_3$ and $\mathbf{e}_1$. It may be added that it was not possible to attribute definitely any of the circulation changes to a lack of observations in the early years or changes in analysis techniques. For example, one might suspect that the pattern of $\mathbf{e}_1$ for July results from early overestimates of the polar anticyclone in summer. If so, the time series of the coefficient of $\mathbf{e}_1$ suggests that the overestimates are largely confined to the second decade of this century.

6. SUMMARY

The forms of the first several eigenvector patterns indicate the geographic regions of greatest year-to-year variability and suggest some spatial associations. While some features of the patterns have been frequently studied, others have not. For example, the possible relationship between changes in the intensity and position of the Aleutian Low and downstream changes over the North Atlantic requires further study. Analysis of time series

of the eigenvector's coefficients permits specification of circulation changes with reference to a particular space scale, namely, that of the major centers of action. Two intervals of change are identified, the early to mid-1920s and the early to mid-1950s. It was not possible to specify these times more precisely. The circulation patterns of the three periods separated by these intervals appear different enough and of sufficient duration to warrant a more complete comparison of the hemispheric climates for each period. Because of the problems of eigenvector interpretation described in section 3 and because only one variable has been treated, this analysis adds little to the physical understanding of circulation variability. It is mainly useful in helping to isolate both spatial regions and times of particular interest that may then be studied by more suitable techniques.

Note added in proof—Additional discussion of techniques for representing spatial and temporal variations of meteorological elements is found in Julian (1970). The quasi-biennial variations in the centers of action have been treated by Angell et al. (1969).

ACKNOWLEDGMENTS

This research was done while the author was at the Meteorological Office, Bracknell, Berkshire, England, supported by a North Atlantic Treaty Organization Postdoctoral Fellowship in Science. Numerical computations were supported by the Atmospheric Science Division, National Science Foundation, Grant GA-10651X, and executed at the University of Wisconsin Computing Center, Madison.

REFERENCES

Angell, J. K., Korshover, J., and Cotton, G. F., "Quasi-Biennial Variations in the 'Centers of Action,'" *Monthly Weather Review*, Vol. 97, No. 12, Dec. 1969, pp. 867–872.

Bjerknes, Jacob, "Synoptic Survey of the Interaction of Sea and Atmosphere in the North Atlantic," *Geofysiske Publikasjoner*, Vol. 24, No. 3, 1962, pp. 116–145.

Bjerknes, Jacob, "A Possible Response of the Atmospheric Hadley Circulation to Equatorial Anomalies of Ocean Temperature," *Tellus*, Vol. 18, No. 4, 1966, pp. 820–828.

Brier, Glenn W., "Long-Range Prediction of the Zonal Westerlies and Some Problems in Data Analysis," *Reviews of Geophysics*, Vol. 6, No. 4, Nov. 1968, pp. 525–551.

Craddock, J. M., and Flood, C. R., "Eigenvectors for Representing the 500 Mb Geopotential Surface Over the Northern Hemisphere," *Quarterly Journal of the Royal Meteorological Society*, Vol. 95, No. 405, July 1969, pp. 576–593.

Dzerdzeevskii, B. C., "Some Aspects of Dynamic Climatology," *Tellus*, Vol. 18, No. 4, 1966, pp. 751–760.

Gilman, Donald L., "Empirical Orthogonal Functions Applied to Thirty-Day Forecasting," *Scientific Report* No. 1, Contract No. AF19(604)-1283, Department of Meteorology, Massachusetts Institute of Technology, Cambridge, June 30, 1957, 129 pp.

Girs, A. A., "On Peculiarities of the Arctic Meteorological Regime in Different Stages of the Circulation Epoch 1949–1964," *WMO Technical Note* No. 87, World Meteorological Organization, Geneva, 1967, pp. 454–477.

Gommel, William R., "Mean Distribution of 500-Mb Topography and Sea-Level Pressure in Middle and High Latitudes of the Northern Hemisphere During the 1950–59 Decade, January and July," *Journal of Applied Meteorology*, Vol. 2, No. 1, Feb. 1963, pp. 105–113.

Hirose, Mototaka, and Kutzbach, John E., "An Alternate Method for Eigenvector Computations," *Journal of Applied Meteorology*, Vol. 8, No. 4, Aug. 1969, p. 701.

Iudin, Mikhail I., "On the Study of Factors Determining the Non-Stationarity of the General Circulation," *Proceedings of the International Symposium on Dynamics of Large-Scale Processes, Moscow, June 23–30, 1965*, Akademiia nauk SSSR, Moscow, 1967, 24 pp.

Julian, Paul R., "An Application of Rank-Order Statistics to the Joint Spatial and Temporal Variations of Meteorological Elements," *Monthly Weather Review*, Vol. 98, No. 2, Feb. 1970, pp. 142–153.

Kutzbach, John E., "Empirical Eigenvectors of Sea-level Pressure, Surface Temperature and Precipitation Complexes Over North America," *Journal of Applied Meteorology*, Vol. 6, No. 5, Oct. 1967, pp. 791–802.

Lamb, Hubert H., *The Changing Climate*, Methuen & Co., Ltd., London, 1966*a*, 236 pp.

Lamb, Hubert H., "Climate in the 1960's: Changes in the World's Wind Circulation Reflected in Prevailing Temperatures, Rainfall Patterns and the Levels of the African Lakes," *Geographical Journal*, Vol. 132, No. 2, June 1966*b*, pp. 183–212.

Lamb, Hubert H., and Johnson, A. I., "Climatic Variation and Observed Changes in the General Circulation," *Geografiska Annaler*, Vol. 41, No. 2/3, 1959, pp. 94–134.

Lamb, Hubert H., and Johnson, A. I., "Secular Variations of the Atmospheric Circulation Since 1750," *Geophysical Memoirs* No. 110, Meteorological Office, London, 1966, 125 pp.

Martin, Donald E., "Anomalies in the Northern Hemisphere 700 Mb 5-Day Mean Circulation Patterns," *Technical Report* No. 105–100, Air Weather Service, U.S. Air Force, Washington, D.C., Apr. 1953, 26 pp.

Namias, Jerome, "Thirty-Day Forecasting—A Review of a Ten-Year Experiment," *Meteorological Monographs*, Vol. 2, No. 6, American Meteorological Society, Boston, July 1953, 83 pp.

Namias, Jerome, "Long Range Weather Forecasting—History, Current Status and Outlook," *Bulletin of the American Meteorological Society*, Vol. 49, No. 5, Part 1, May 1968, pp. 438–470.

Namias, Jerome, "Seasonal Interactions Between the North Pacific Ocean and the Atmosphere During the 1960's," *Monthly Weather Review*, Vol. 97, No. 3, Mar. 1969, pp. 173–192.

Sellers, William D., "Climatology of Monthly Precipitation Patterns in the Western United States, 1931–1966," *Monthly Weather Review*, Vol. 96, No. 9, Sept. 1968, pp. 585–595.

Walker, Gilbert T., and Bliss, E. W., "World Weather V," *Memoirs of the Royal Meteorological Society*, Vol. 4, No. 36, London, Oct. 1932, pp. 53–84.

Willett, H. C., "Solar-Climatic Relationships in the Light of Standardized Climatic Data," *Journal of the Atmospheric Sciences*, Vol. 22, No. 2, Mar. 1965, pp. 120–136.

[*Received November 24, 1969; revised February 27, 1970*]